

Modeling of the surface induction hardening process

Streszczenie. Omówiono zagadnienie modelowania matematycznego hartowania indukcyjnego powierzchniowego. Model ogólny uwzględnia sprzężenie pola elektromagnetycznego, temperaturowego, naprężeń cieplnych i zjawisk metalurgicznych. Badaniom poddano koło zębate wykonane ze stali 50CrMo4. Omówiono wyniki obliczeń i pomiarów rozkładu temperatury po nagrzewaniu indukcyjnym. (Modelowanie matematyczne procesu nagrzewania indukcyjnego powierzchniowego)

Abstract. Mathematical modeling of induction surface hardening was described. The general model takes into consideration coupled electromagnetic, temperature, heat stress and metallurgical fields. As an illustrative example a gear wheel made from steel 50Cr Mo4 was taken. Results of computations and measurements of temperature distribution after induction heating were discussed.

Słowa kluczowe: nagrzewanie indukcyjne, hartowanie powierzchniowe, modelowanie matematyczne, temperatury krytyczne
Keywords: induction heating, surface hardening, mathematical modeling, critical temperatures

doi:10.12915/pe.2014.02.01

Introduction

Surface hardening is the heat treatment process consisting of the rapid heating of the surface layer of the element to a predetermined temperature T_H and then quick enough cooling in order to obtain a martensitic structure in a thin surface zone. This type of heat treatment leads to an increase in surface hardness, wear resistance and fatigue strength while keeping the soft core. In commercial practice, the most common is the induction surface hardening. This process is characterized by a short heating time, low oxidation and decarburization of the treated surface. It is easy to control a thickness of hardened layer by changing the field current frequency. The process is characterized also by the low environmental impact and the ability to automate the process [1].

General model of induction surface hardening

There is a very high heating rate characteristic for the induction heating of steel bodies (in some cases even considerably above 1000 °C /s [2]). It causes a distinct increase in temperature (with respect to the equilibrium temperature) both the beginning and the end of the Ac3 transformation temperature. At high speed of heating the appropriate steel hardening temperature may be distinctly (up to 100 - 200 °C in some cases) higher than the critical temperatures used in the conventional heat treatment [2].

A factor conducive to the application of new technologies of the surface induction hardening to industry, is continuous improvement of methods of mathematical modeling of the process. In recent years, significant progress was made in the study of relations between process parameters and hardness distribution and structure of the hardened layer. Still, the weakness, that negatively affects the accuracy of the mathematical modeling of the process of the steel surface induction hardening, is insufficient knowledge of the phenomena associated with heat transfer. Difficulties with the proper describing of the temperature field occur during the rapid induction heating and both natural and intensive cooling. Determination of

the field with reasonable accuracy is a necessary condition for more precise computer modeling of the induction hardening process. It is also necessary to take into account the fact that in the conditions of induction hardening the body is to be heated to a much higher temperature than in the case of the classical process.

A mathematical model of the process includes an analysis of the coupled electromagnetic, temperature, thermal stress fields and structural transformations during three consecutive stages: induction heating, natural, slow cooling in temperature higher than the austenitization temperature and finally intensive cooling. The block scheme presenting a general view of the model is showed in Fig. 1.

First input data were collected. There were taken from suitable databases or directly determined by measurements. The induction heating process was modeled taking into consideration coupled electromagnetic, temperature and thermal stresses phenomena. Non-linear dependence of material properties on temperature were taken into account. Then non-stationary temperature for a (1) short period of natural cooling were calculated. The next step was the quenching where the hardened body was intensively cooled. It requires calculation of coupled temperature, thermal stresses and metallurgical fields. The results of computations was hardness distribution determined based upon experimental data taken from measurements provided for samples of investigated steel. If a final criteria were satisfied the computations were finished, otherwise the computations were repeated for a modified model.

Mathematical modeling

The electromagnetic field is described classically by means of the magnetic vector potential A :

$$(1) \quad \text{curl} \frac{1}{\mu} \text{curl} A + \gamma(\mathbf{v} \times \text{curl} A) = \mathbf{J}_z$$

where: μ - denotes the magnetic permeability, γ - electrical conductivity, \mathbf{v} - the velocity of the inductor in relation to the workpiece, \mathbf{J}_z - the field current density.

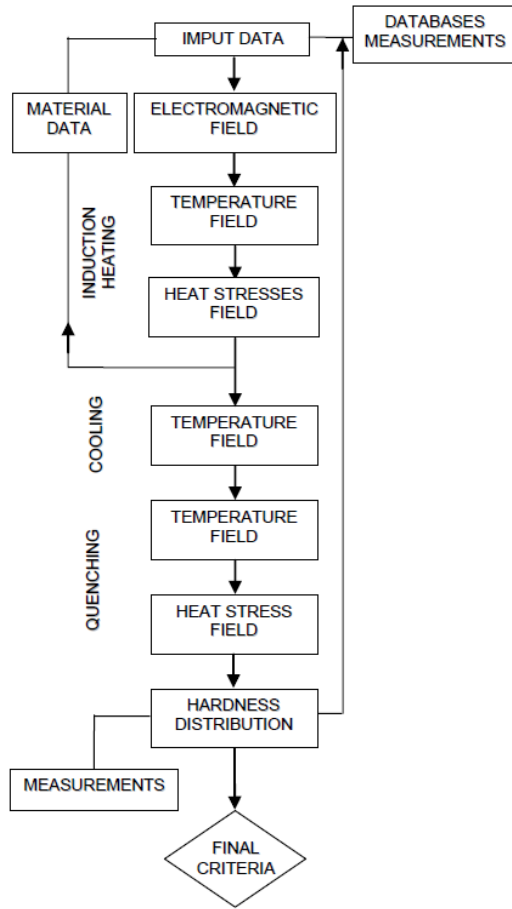


Fig.1. The general model of the induction surface hardening

The solution of (1) is still a challenge especially in case of coupled electromagnetic-thermal problem analysis. A reason of that should be for instance disproportion between field current frequency and time constant for temperature field. Due to that a simplified model dealing with harmonic approach is mostly introduced. The magnetic permeability of any ferromagnetic parts is not supposed to be a constant. It is a function of local value of the module of the magnetic flux density $|\mathbf{B}|$ in the ferromagnetic sub-domain. The equation (1) is transformed to the form (2) for the phasor of the magnetic vector potential $\underline{\mathbf{A}}$:

$$(2) \quad \text{curl curl } \underline{\mathbf{A}} + j\omega\mu\gamma \underline{\mathbf{A}} - \mu\gamma(\mathbf{v} \times \text{curl } \underline{\mathbf{A}}) = \mu \underline{\mathbf{J}}_z$$

where: j - is the imaginary unit, and ω - the angular frequency.

Third left-hand term of equation (2) can be omitted because of a small velocity of movement and high frequencies of the field current, which actually is mostly applied for the surface induction hardening process [3].

The phasor of eddy currents induced in the charge is given by (3)

$$(3) \quad \underline{\mathbf{J}} = j\omega\gamma \underline{\mathbf{A}},$$

These eddy-currents generate local volumetric Joule losses being the local heat source. The time- average value of them are given by (4)

$$(4) \quad p_v = \frac{1}{2} \cdot \frac{\underline{\mathbf{J}} \cdot \underline{\mathbf{J}}^*}{\gamma}$$

where $\underline{\mathbf{J}}^*$ conjugate to the phasor $\underline{\mathbf{J}}$ represented by its maximal value

In case of induction heating of ferromagnetic bodies there are some additional losses connected with magnetic hysteresis phenomena. Their value is distinctly smaller and they were neglected.

Temperature field is determined based on the Fourier-Kirchhoff equation supplemented by the term representing the time-average value of the volumetric Joule losses taken from the electromagnetic field calculations.

$$(5) \quad \text{div}(\lambda \text{grad} T) - \rho c(\mathbf{v} \text{grad} T) - \rho c \frac{\partial T}{\partial t} = -p_v$$

where: λ - thermal conductivity, ρ - density, c - specific heat.

For accurate simulation of the temperature field a crucial was the proper formulation of the third kind of the boundary condition, which should take into consideration not only the convection heat transfer but also the radiation heat transfer with multiple reflection phenomena [3]:

$$(6) \quad -\lambda \frac{\partial T}{\partial n} = \alpha_c(T - T_c) + \sigma_0 \cdot \varepsilon \cdot (T^4 - T_r^4) = \alpha_c(T - T_c) + \alpha_r(T^4 - T_r^4) - p_r$$

where: α_c - convection heat transfer coefficient, T_c - temperature of convection environment, σ_0 - Stefan-Boltzmann constant, ε - total emissivity, T_r - temperature of the surrounding radiation environment, α_r - radiation heat transfer coefficient, p_r - surface density of power component associated with the multiple reflections phenomena.

Often, it can be assumed that $T_c \approx T_r = T_{cr}$ and do not take into consideration the effect of multiple reflections, the boundary condition (5) takes the form of:

$$(7) \quad -\lambda \frac{\partial T}{\partial n} = \alpha_g(T - T_{cr}),$$

$$\alpha_g = \alpha_c + \sigma_0(T^2 - T_{cr}^2) \cdot (T - T_{cr})$$

where: α_g - the equivalent heat transfer coefficient, T_{cr} - the average temperature of the surrounding environment.

Both thermal stresses and thermal deformations field is described by the Lamé equations for displacements [5].

$$(8) \quad (\phi_u + \psi_u) \text{grad div } \mathbf{u} + \psi_u \nabla^2 \mathbf{u} - (3\phi_u + 2\psi_u) \alpha_T \text{grad } T + \mathbf{f}_m = 0$$

where: ϕ_u, ψ_u - factors defined by (9), \mathbf{u} - vector of displacements, α_T - linear expansion coefficient, \mathbf{f}_m - density of Lorentz force expressed by the equation (10) for maximal values of phasors:

$$(9) \quad \varphi_u = \frac{\nu \cdot E}{(1+\nu) \cdot (1-2\nu)}, \quad \psi_u = \frac{E}{2(1+\nu)}$$

where: ν – kinematic viscosity, E – Young's modulus.

$$(10) \quad f_m = \frac{1}{2} \operatorname{Re}\{\underline{J} \times \underline{B}\}$$

For the case of the surface induction hardening of gear wheels the displacements were minimal and could be neglected.

Illustrative example

Both the material properties and their dependence on temperature and as well the hardening temperature T_h were determined by measurements. Based upon the provided measurements the TTA (Time -Temperature-Austenitization) diagram was determined [2]. Then the dependence of the upper critical temperature A_{c3} on speed of heating was calculated (Fig. 2).

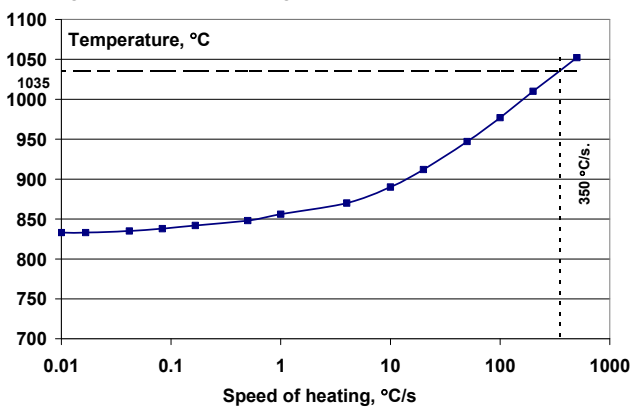


Figure 2. Dependence of the upper critical temperature A_{c3} on speed of heating [2]

Based upon these data the hardening temperature ($T_h = 1085$ °C) was chosen. It was bigger than the upper critical temperature ($A_{c3} = 1035$ °C) at 50 °C. The measurement results confirmed that, for induction heating process, hardening temperature has to be increased significantly above the value T_h used in conventional technologies. There were examined a gear wheel (Fig. 3) made of steel 50 CrMo4.

The outer diameter of the gear wheel is 45.7 mm, number of teeth – 41. Induction hardening was performed simultaneously by using the single-coil cylindrical inductor with the inner diameter of 54 mm (see Fig. 4). As a quenchant sprayed water was used. The sprayer was constructed in the form of a ring having the inner diameter of 80 mm.

Calculations and measurements

The calculations were performed by means of the software package FLUX 3D. The resulting calculation of the temperature distribution after induction heating ($t = 3$ s) along the inner surface of the tooth shown in Figure 4. Even for the smallest value of the field current $I = 2300$ A over the entire working surface of the tooth a temperature higher than the desired hardening temperature was obtained.

a)



b)

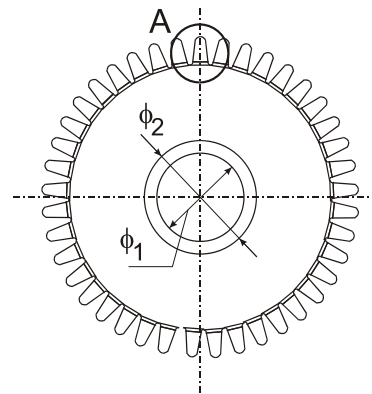


Fig. 3. Gear wheel. View (a) and drawing (b) with an indication A of the calculation area [5]

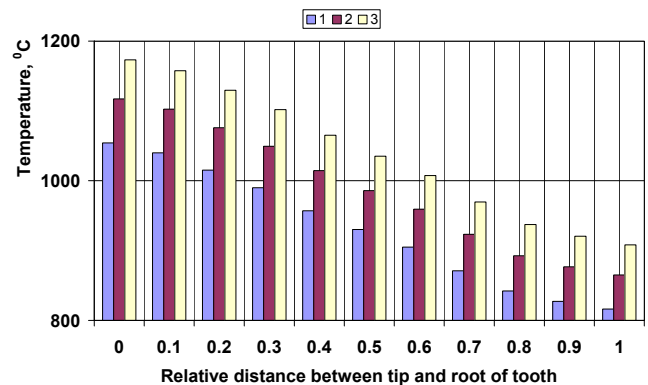


Fig.4. Temperature distribution along the surface of the tooth after the induction heating for different field current, (1 - $I = 2300$ A, 2 - $I = 2400$ A, 3 - $I = 2500$ A)

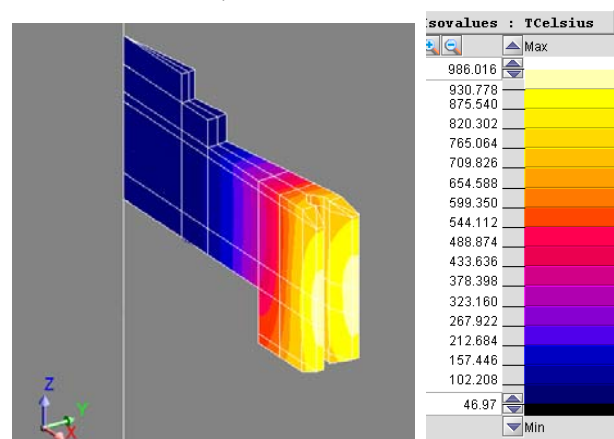


Fig. 5 The calculated temperature distribution after 3 seconds of induction heating

In order to verify calculation results an experimental stand for surface induction hardening was built. Its more detailed description was presented in [6]. The stand was installed in the laboratory of the ELKON company in Rybnik [7]. The view of the stand was shown in Fig.6.

A satisfactory convergence between the calculation results and measurements was obtained. Some aspects of induction surface hardening of gear wheels were undertaken as well in some other papers written by researchers from the Department of the Industrial Informatics of the Silesian University of Technology, for instance in [8 - 9].



Fig. 6. Experimental stand 1 – gear wheel, 2 – inductor with connections, 3 - sprayer

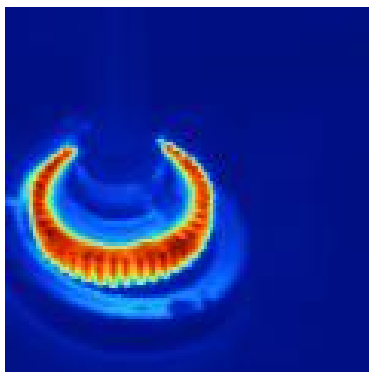


Fig. 7 The temperature distribution after 3 seconds heating measurement results

Conclusions

The paper presents a general description of the mathematical modeling of the surface induction hardening process. The illustrative example deals with the contour induction surface hardening of gear wheels made from steel 50CrMo4. The influence of speed of induction heating to the values of criteria temperatures was analyzed. The 3D calculations of coupled electromagnetic and temperature fields during induction heating were compared with the measurements. Quite reasonable accuracy was achieved. Next activities in the domain should be aimed to improvement of numerical algorithms making possible to increase accuracy and decrease the total time of calculations.

Acknowledgement

The paper was prepared with a financial support with the research projects NN510256338 and BK-343/RM4/2012 sponsored by the Ministry of Science and Higher Education.

REFERENCES

- [1] Rudnev, V., D. Loveless, R. Cook and M. Black. Handbook of Induction Heating, Marcel Dekker Inc., New York, (2003)
- [2] Barglik J., Ducki K, Hering M. and others: Modeling of induction hardening proces of steel elements surfaces with taking into consideration radiation heat transfer phenomena. KBN T08C 016 30 (2006) (in Polish)
- [3] Barglik J., Doležel I., Ulrych B.: Induction heating of moving bodies. Proceedings of the International Conference „SPETO” (1999) pp.167-170
- [4] Barglik J., Czerwiński M., Hering M., Wesolowski M.: Radiation in Modelling of Induction Heating Systems, IOS Press Amsterdam, Berlin, Oxford, Tokyo, Washington DC, (2008), 202-211
- [5] Orłoś Z.: Heat stresses, PWN, 1991
- [6] Smalcerz A., Przyłucki R., Konopka K., Fornalczyk A., Ślęzak M.: Multi-variant calculations of induction heating process, Archives of Materials Science and Engineering, 58 (2012), nr 2, 177-181
- [7] www.elkon.com.pl
- [8] Niklewicz M., Smalcerz, A. Kurek A.: Estimation of system geometry and inductor frequency importance in induction hardening process of gears, Przegląd Elektrotechniczny, 11, (2008), 219-224
- [9] Przyłucki, R., Smalcerz, A.: Induction heating of gears - pulsing dual-frequency concept, Metalurgija. 52 (2013), nr 2, 235-238,

Authors of the paper: prof. nzw. dr hab. inż. Jerzy Barglik., Silesian University of Technology, Faculty of Material Science and Metallurgy, Department of Industrial Informatics ul. Krasińskiego 8, 40-019 Katowice, E-mail: jerzy.barglik@polsl.pl; prof. dr hab. Tadeusz Wieczorek, Silesian University of Technology, Faculty of Material Science and Metallurgy, Department of Industrial Informatics, ul. Krasińskiego 8, 40-019 Katowice, E-mail: tadeusz.wieczorek@polsl.pl; dr inż. Albert Smalcerz, Silesian University of Technology, Faculty of Material Science and metallurgy, Department of Industrial Informatics ul. Krasińskiego 8, 40-019 Katowice, albert.smalcerz@polsl.pl;